

AD-A054 217

COLD REGIONS RESEARCH AND ENGINEERING LAB HANOVER N H
IN-PLANE DEFORMATION OF NON-COAXIAL PLASTIC SOIL (U)
APR 78 S TAKAGI
CRREL-78-7

F/G 8/13

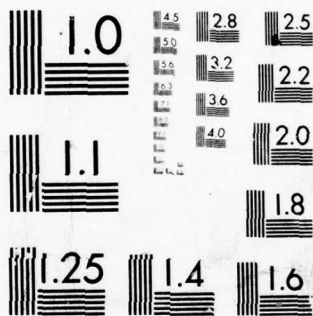
UNCLASSIFIED

NL

| OF |
AD
A054217



END
DATE
FILMED
6-78
DDC



MICROCOPY RESOLUTION TEST CHART
NATIONAL BUREAU OF STANDARDS-1963-A

CRREL REPORT 78-7

FOR FURTHER TRAN

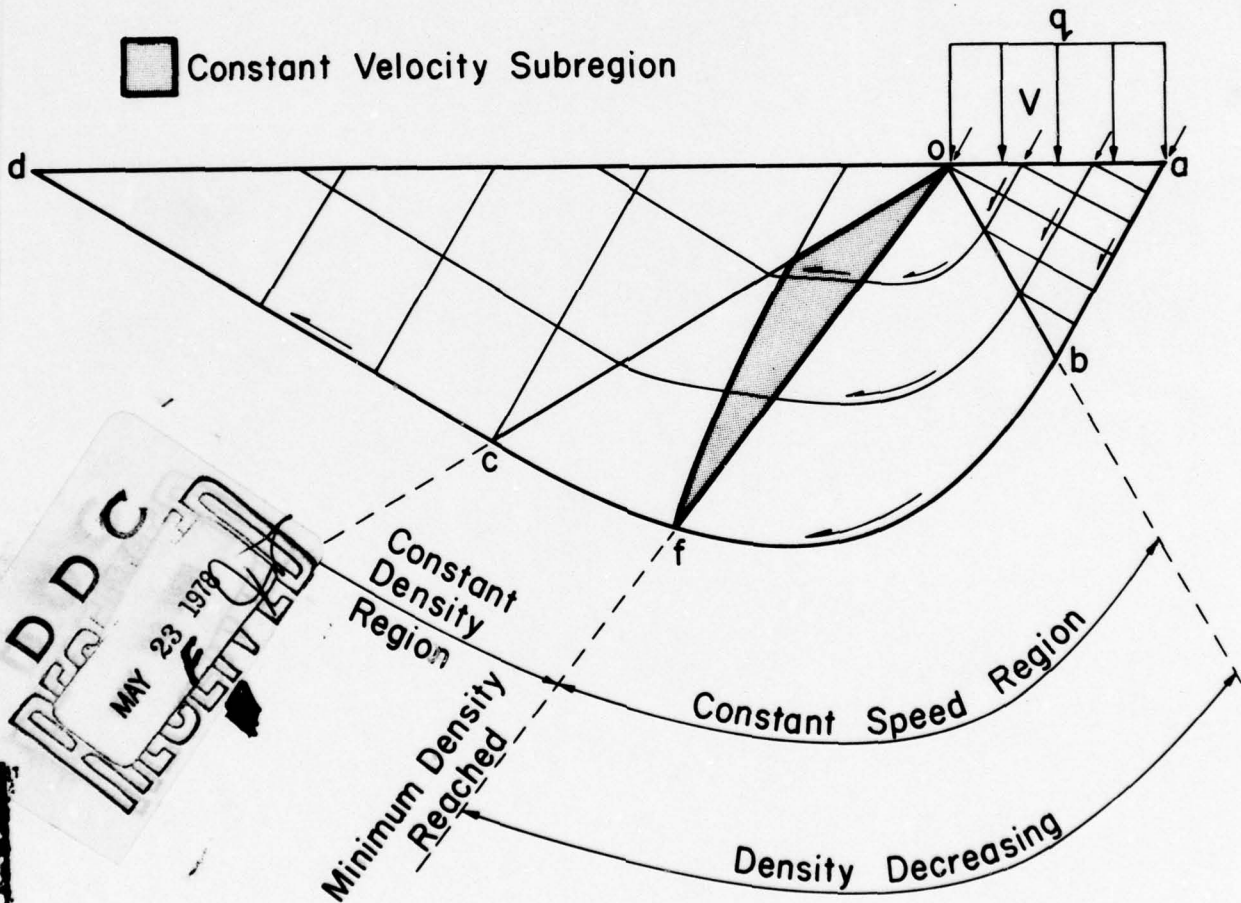
12



In-plane deformation of non-coaxial plastic soil

AD A 054217

□ Constant Velocity Subregion



DDC
MAY 23 1978
RECEIVED

DDC FILE COPY

This document has been approved for public release and sale; its distribution is unlimited.

*Cover: Net of stress characteristic lines in the ground
sustaining a rectangular load.*

CRREL Report 78-7

In-plane deformation of non-coaxial plastic soil

Shunsuke Takagi

April 1978

Prepared for
DIRECTORATE OF FACILITIES ENGINEERING
OFFICE, CHIEF OF ENGINEERS

By
CORPS OF ENGINEERS, U.S. ARMY
COLD REGIONS RESEARCH AND ENGINEERING LABORATORY
HANOVER, NEW HAMPSHIRE

Approved for public release; distribution unlimited

Unclassified

SECURITY CLASSIFICATION OF THIS PAGE (When Data Entered)

REPORT DOCUMENTATION PAGE		READ INSTRUCTIONS BEFORE COMPLETING FORM
1. REPORT NUMBER 14 7 CRREL- 78-7	2. GOVT ACCESSION NO.	3. RECIPIENT'S CATALOG NUMBER
6 4. TITLE (and Subtitle) IN-PLANE DEFORMATION OF NON-COAXIAL PLASTIC SOIL	5. TYPE OF REPORT & PERIOD COVERED	
	6. PERFORMING ORG. REPORT NUMBER	
7. AUTHOR(s) 10 Shunsuke Takagi	8. CONTRACT OR GRANT NUMBER(s)	
9. PERFORMING ORGANIZATION NAME AND ADDRESS U.S. Army Cold Regions Research and Engineering Laboratory Hanover, New Hampshire 03755	10. PROGRAM ELEMENT, PROJECT, TASK AREA & WORK UNIT NUMBERS 16 DA Project 4A161102AT24 Task A1, Work Unit 002 17 A1	
	11. CONTROLLING OFFICE NAME AND ADDRESS Directorate of Facilities Engineering Office, Chief of Engineers Washington, D.C. 20314 11	12. REPORT DATE Apr 78
14. MONITORING AGENCY NAME & ADDRESS (if different from Controlling Office)	13. NUMBER OF PAGES 31	
	15. SECURITY CLASS. (of this report) Unclassified 12 33 p.	
15a. DECLASSIFICATION/DOWNGRADING SCHEDULE		
16. DISTRIBUTION STATEMENT (of this Report) Approved for public release; distribution unlimited.		
17. DISTRIBUTION STATEMENT (of the abstract entered in Block 20, if different from Report)		
18. SUPPLEMENTARY NOTES		
19. KEY WORDS (Continue on reverse side if necessary and identify by block number) Continuum mechanics In-plane deformation Non-coaxiality Plastic soils Soil mechanics		
20. ABSTRACT (Continue on reverse side if necessary and identify by block number) The theory of non-coaxial in-plane plastic deformation of soils that obey the Coulomb yield criterion is presented. The constitutive equations are derived by use of the geometry of the Mohr circle and the theory of characteristic lines. It is found that, for solving a boundary value problem, the non-coaxial angle must be given such values that enable us to accommodate the presupposed type of flow in the given domain satisfying the given boundary conditions. The non-coaxial angle is contained in the constitutive equations as a parameter. Therefore, the plastic material obeying the Coulomb yield criterion is a singular material whose constitutive equations are not constant with material but are variable with flow conditions.		

DD FORM 1 JAN 73 1473

EDITION OF 1 NOV 65 IS OBSOLETE

Unclassified

SECURITY CLASSIFICATION OF THIS PAGE (When Data Entered)

037 100

Sm

PREFACE

This report was prepared by Dr. Shunsuke Takagi, Research Physical Scientist, of the Physical Sciences Branch, Research Division, U.S. Army Cold Regions Research and Engineering Laboratory.

The study covered by this report was performed under DA Project 4A161102AT24, *Research in Snow, Ice and Frozen Ground*; Task A1, *Properties of Cold Regions Materials*; Work Unit 002, *Properties of Frozen Soil*.

This report was technically reviewed by Dr. Y.C. Yen and R. Johnson of CRREL.

CONTENTS

	Page
Abstract	i
Preface	ii
Introduction	1
Analysis of stress	2
Geometry of the Mohr circle	2
Stress characteristic directions	3
Analysis of strain rate	4
Constitutive equations	4
Strain-rate characteristic directions	7
Constitutive geometry	8
Strain-rate tensor	10
The dyadic expression	10
Plastic work rate	13
Coordinate transformation	13
Example	15
The stress solution	15
Velocity equations in the σ -characteristic curvilinear coordinates	16
The constant speed solution	19
Velocity equations in the constant density region	21
Solution in the first constant-density subregion	22
Solution in the second constant-density subregion	23
Solution in the passive region	25
Conclusion	26
Literature cited	27

ILLUSTRATIONS

Figure	
1a. Pole on the stress plane	3
1b. Tangential stress in the physical plane	3
2. Stress characteristic directions	4
3. Strain rate Mohr circle superimposed on the stress Mohr circle	5
4a. Geometry of the $+m$ coincidence	9
4b. Geometry of the $-m$ coincidence	9
5a. Domains $\dot{\epsilon}_{\text{max}}^T = 0$ on the Mohr circle — the case of $+m$ coincidence	11
5b. Domains $\dot{\epsilon}_{\text{min}}^T = 0$ on the Mohr circle — the case of $-m$ coincidence	11
6a. A net of stress characteristic lines in the ground sustaining a rectangular load	15
6b. Geometry of the characteristic directions of Figure 6a	15
7. The first and second subregions of the constant density region	23
8. Solution in the second subregion	24
9. Velocity field in the passive region	25

TABLES

Table	
I. Velocity components on the boundaries of the passive region	26

ACCESSION for	
NTIS	<input checked="" type="checkbox"/>
DDC	<input type="checkbox"/>
UNANNOUNCED JUSTIFICATION	<input type="checkbox"/>
BY _____	
DISTRIBUTION/AVAILABILITY CODES	
Dist.	AVAIL. and/or SPECIAL
A	

IN-PLANE DEFORMATION OF NON-COAXIAL PLASTIC SOIL

Shunsuke Takagi

INTRODUCTION

The work on mathematical soil plasticity started with Drucker and Prager,⁷ Shield,¹⁷ following their theory, showed some typical solutions of the in-plane deformation. However, the plastic deformation defined by these authors is always accompanied by dilatancy, and deviates from the slip direction by a definite angle. The solution of the deformation derived by them does not satisfy the boundary slip-line condition that imposes restrictions on both stress and flow.

Haythornthwaite,¹⁰ DeJosselin de Jong,⁴ and Mandl¹² expressed suspicion and suggested ways of modifying Drucker and Prager's implicit assumption that the stress and strain rate tensors are coaxial. If the coaxiality is no longer true, the strain-rate tensor is not normal to the yield criterion surface in the six-dimensional stress space, and the theory of plastic potential (Drucker,⁵ Drucker,⁶ p. 273) cannot be used to derive the constitutive equations. Then, the basic premise of Drucker and Prager's⁷ development does not hold.

On the other hand, Geniev⁸ formulated a theory of in-plane deformation assuming that the non-coaxial angle is equal to one half the frictional angle. The deformation he formulated causes no volume change. We²⁰ extended the non-coaxial angle to an arbitrary value. The deformation we formulated can accommodate both dilatancy and compression. However, introduction of the unknown non-coaxial angle increases the number of unknowns by one; no method of evaluating the non-coaxial angle has ever been discovered, and no boundary-value problem has ever been solved. This difficulty is now overcome. We discovered that the non-coaxial angle must be so determined that the presupposed flow can be accommodated in the given domain satisfying the given boundary conditions.

In the following, first we introduce the geometry of the Mohr circle, which is developed into a complete mathematical tool compatible with the analytical method. This is achieved by introducing the sign of tangential components, called *sign m*, which we believe will find applications also in other branches of mechanics than in soil mechanics.

Second, we derive the constitutive equations by applying the geometry of the Mohr circle and the theory of the characteristic lines. In our theory, it is not required that both of the strain-rate characteristic directions be coincident with both of the stress characteristic directions. For a plastic deformation to occur, it is sufficient that one member in a set of strain-rate characteristic directions be coincident with the same *sign m* member of the stress characteristic directions. The coincident and noncoincident directions are called *doublet* and *singlet*, respectively. In this way, we formulate the *volume characteristic equation*, which shows that either volume expansion, shrinkage, or no volume change can occur in accordance with the value of the non-coaxial angle. Introduction of this equation enables us to complete the formulation of the constitutive equations.

The differential equations for solving a boundary value problem in this paper are derived by use of the following property of the strain-rate characteristic lines: the lengths of the curve elements of the strain-rate characteristic lines are maintained constant during the plastic deformation. The expression of this fact, or more in general, the expression of the components of the simplified

strain-rate tensor, by use of an appropriately chosen coordinate system gives the differential equations for solving a deformation boundary value problem. The differential equations contain the non-coaxial angle, to which we can assign an appropriate value so that the presupposed type of flow can be fitted into the given domain. As an example, Hill's¹¹ solution of the stress distribution in the ground sustaining a rectangular load is given a deformation solution. The solution presented here is the simplest one that can be fitted into the given domain of the stress solution.

We introduce the term *Coulomb material* to designate the non-coaxial plastic material that obeys the Coulomb yield criterion in the in-plane deformation. The concept of Coulomb material enables us, we believe, to start the rational mechanics formulation of soil deformation. However, before we can discover a satisfactory model of soil deformation, we must endow the Coulomb material with some more rational mechanics concepts, as discussed in the conclusion of this report.

In this report, we have revised several concepts, improved the terminology, and corrected mistakes in our previous papers.^{19 20 23}

ANALYSIS OF STRESS

Geometry of the Mohr circle

Terzaghi²⁴ introduced the concept of pole on the Mohr circle to describe the orientation of a stress tensor in the physical plane. In Figure 1a, A and B are the points expressing the major and minor principal stresses, σ_1 and σ_2 , respectively. In the physical plane, there exists a pair of lines on which σ_1 and σ_2 work. (They are shown by $A_1 Q_1$ and $B_1 Q_1$ on the right side of Figure 1b, and by $A_2 R_2$ and $B_2 R_2$ on the left side, respectively.) Let us draw lines AP and BP parallel to the lines on whose normal directions σ_1 and σ_2 , respectively, work. The lines AP and BP intersect at point P on the Mohr circle, which is called *pole*. Pole has the following property (Terzaghi,²⁴ p. 18): Let Q be a point on the Mohr circle representing stress (σ, τ) . Then, line PQ is parallel to a physical line on which the stress (σ, τ) in the physical plane works.

Locating the stress point on either the upper or the lower semicircle is essentially important to the geometry of the Mohr circle. In the following, an effective method that enables us to decide the location of the stress point will be presented.

First, we consider a point Q on the upper semicircle in Figure 1a. We draw, as shown in the right side of Figure 1b, $Q_1 A_1$, $Q_1 B_1$, and $A_1 B_1$ parallel to PA, PB, and PQ. Note that the hypotenuse $A_1 B_1$ is parallel to the physical line under consideration. The tangential stress τ on both sides of $A_1 B_1$ makes the rotational direction as shown, as may be verified by decomposing σ_1 and σ_2 in the directions parallel and normal to $A_1 B_1$. To designate the sign of τ , we suppose that a pair of τ 's on both sides of $A_1 B_1$ form a couple. We find that the fictitious couple formed by the tangential stress components makes the counterclockwise rotational direction.

Second, we consider point R on the lower semicircle of Figure 1a. Repeating the similar procedure, as shown on the left of Figure 1b, we find that the fictitious moment formed by a pair of τ 's on both sides of $A_2 B_2$, $A_2 B_2$ being parallel to PR, makes the clockwise rotational direction.

The direction of τ thus defined is convenient for locating a stress point on the Mohr circle. Let us suppose a fictitious tangential-stress moment formed by the slipping motion on a slip-line boundary; then, we can locate the stress point of a slip-line boundary on the Mohr circle (see Fig. 6a and 6b). This clue usually enables us, even prior to solving the problem, to locate the stress points of the entire region on the Mohr circle.

The counterclockwise and clockwise rotational directions of the fictitious moment are called *sign +m* and *-m*, respectively.^{19 20} The *+m* and *-m* stress points are on the upper and lower semicircles, respectively, of the stress Mohr circles.

The geometry of the Mohr circle thus amplified with the introduction of the sign of tangential components may be used for any second-order symmetric tensors. It is a complete mathematical tool that is compatible with the analytical method, as shown in the following applications.

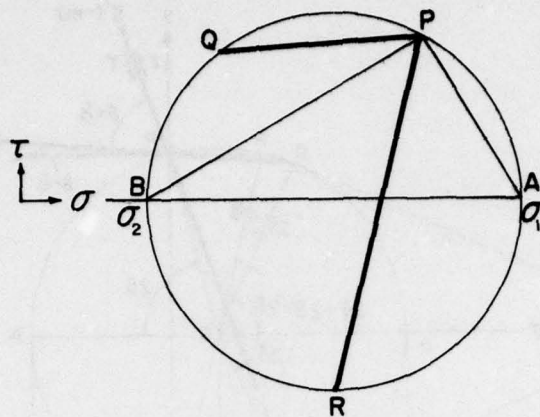


Figure 1a. Pole on the stress plane.

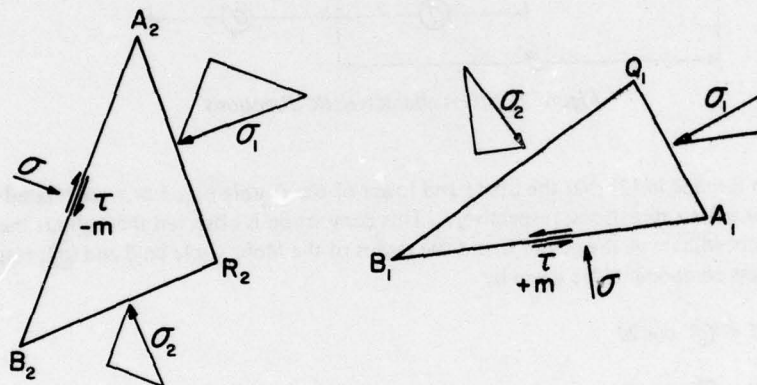


Figure 1b. Tangential stress in the physical plane.

Stress characteristic directions

We shall formulate stress characteristic directions by use of the geometry of the Mohr circle.

In Figure 2, PD and PE are the $+m$ and $-m$ σ -characteristic directions. (We reserve the term slip for a later use, because slip implies more than a stress state.) We designate by 2θ the central angle ACP, where C is the center of the Mohr circle. We take the right-hand coordinate system x, y , as shown with the origin located at P, where the x -axis is drawn parallel to the axis ACB. When used to locate a point on the circle, a central angle in the counterclockwise direction is positive in the right-hand coordinate system. We introduce the complementary frictional angle δ by

$$2\delta = \pi/2 - \rho \quad (1)$$

where ρ is the frictional angle of the soil under consideration. We denote by H and V the points at which the opposite extensions of the x and y -axes intersect with the circle, respectively. Then the angles HPD and HPE are half the central angles HCD and HCE, respectively. Thus we find

$$\frac{dy}{dx} = \tan(\theta \mp \delta). \quad (2)$$

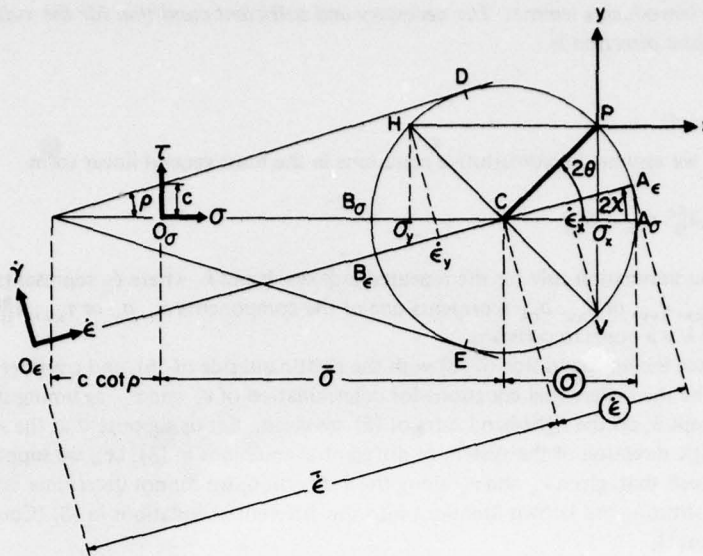


Figure 3. Strain-rate Mohr circle superimposed on the stress Mohr circle.

We consider a strain-rate Mohr circle determined in response to the stress Mohr circle. Let us superimpose, as shown in Figure 3, the strain-rate Mohr circle on the stress Mohr circle, by, if necessary, changing the scale, moving the origin, and rotating the axis of the strain-rate Mohr circle, so that the pole of the latter falls on the pole of the former. In Figure 3, the axis $A_\epsilon C B_\epsilon$ of the strain-rate Mohr circle is rotated by angle 2χ from the axis $A_\sigma C B_\sigma$ of the stress Mohr circle, where χ denotes the non-coaxial angle. The origin of the $\dot{\epsilon}$, $\dot{\gamma}$ coordinates is at O_ϵ . The strain-rate Mohr circle of zero-length radius is excluded from this operation.

First, let us formulate the strain rate components. Let the $\dot{\epsilon}$ -coordinate of the center C and the radius of the strain rate Mohr circle be $\bar{\epsilon}$ and ϵ , respectively; ϵ is positive, but $\bar{\epsilon}$ can be positive, zero, or negative. The values of $\dot{\epsilon}_x$ and $\dot{\epsilon}_y$ are given by the intersection of axis $A_\epsilon C B_\epsilon$ with the normals drawn from V and H to $A_\epsilon C B_\epsilon$, respectively. Then, by using the relation $\angle VCA_\sigma = 2\theta$, we find

$$\begin{aligned}\dot{\epsilon}_{xx} &= \bar{\epsilon} + \epsilon \cos(2\theta + 2\chi) \\ \dot{\epsilon}_{yy} &= \bar{\epsilon} - \epsilon \cos(2\theta + 2\chi) \\ \dot{\epsilon}_{xy} &= \epsilon \sin(2\theta + 2\chi).\end{aligned}\tag{5}$$

Let v_x and v_y be the x - and y - components of the velocity v . We define the compression to be positive; then,

$$\begin{aligned}\dot{\epsilon}_{xx} &= -\frac{\partial v_x}{\partial x} \\ \dot{\epsilon}_{yy} &= -\frac{\partial v_y}{\partial y} \\ \dot{\epsilon}_{xy} &= -\frac{1}{2} \left(\frac{\partial v_x}{\partial y} + \frac{\partial v_y}{\partial x} \right).\end{aligned}\tag{6}$$

Second, we introduce a lemma: *The necessary and sufficient condition for the x-direction to be an $\dot{\epsilon}$ -characteristic direction is*

$$\dot{\epsilon}_x = 0. \quad (7)$$

To prove this, we assume the constitutive equations in the most general linear form

$$\dot{\epsilon}_{ij} = \lambda(A_{ij}^{hk} \sigma_{hk} + B_{ij}) \quad (8)$$

by applying the summation rule for the repeated indexes, h and k , where $\dot{\epsilon}_{ij}$ represents one of the components $\dot{\epsilon}_{xx}$, $\dot{\epsilon}_{yy}$, or $\dot{\epsilon}_{xy}$; σ_{hk} represents one of the components σ_x , σ_y or τ_{xy} ; A_{ij}^{hk} and B_{ij} are constants; and λ is a nonzero constant.

Let us replace the left-hand side of (8) with the right-hand side of (6), and consider the equations thus found to be the differential equations for determination of v_x and v_y , assuming that all the quantities, except λ , on the right-hand sides of (8) are given. Let us suppose that the x -direction is the characteristic direction of the system of differential equations in (8); i.e., we suppose that the x -direction is such that, given v_x and v_y along the x -direction, we cannot determine $\partial v_x / \partial y$ or $\partial v_y / \partial y$ by substituting the known functions into the differential equations in (8) (Courant and Hilbert,³ Abbott¹).

If $\dot{\epsilon}_{xx}$ is not zero, the equation of $\dot{\epsilon}_{xx}$ in (8) can be used to determine λ , because λ is the only one unknown in this equation. If (7) is correct, the right-hand side of the equation of $\dot{\epsilon}_{xx}$ in (8) must be equal to zero, because this equation is an identity; therefore, λ is indeterminate. Then, $\partial v_x / \partial y$ and $\partial v_y / \partial y$ are also indeterminate. Equation (7) is therefore the necessary and sufficient condition. The lemma is thus proved. We shall later show that we can actually arrive at the constitutive equations in the form of (8).

Third, we introduce the *principle of partial coincidence* as a requirement for a plastic deformation to occur. In the conventional theory of plasticity, it is postulated that both of the stress-characteristic directions are coincident with both of the strain-rate characteristic directions. However, the coincidence of both of the characteristic directions is not necessary. We postulate that, for a plastic deformation to occur, one member of a set of directions must be coincident with the member of the same sign m in the other set. If one member is coincident, the boundary flow conditions and the boundary stress conditions can be met along the coincident direction. If there is no coincident direction, it is impossible to connect the two sets of discontinuous solutions across a line.

The coincident and noncoincident directions are called *doublet* and *singlet*, respectively. There are two singlets: a σ -singlet and an $\dot{\epsilon}$ -singlet. When the doublet has sign $+m$ or $-m$, we say that the $+m$ or $-m$ coincidence has occurred. Finally, if velocity is in the doublet direction, we call the flow line a *slip line*.

Fourth, let us resume the interpretation of (7). We assume that the x -direction is the doublet; then, in accordance with the $+m$ or $-m$ coincidence, the x -direction must be either PD or PE in Figure 2. Then, from the geometry, θ must be equal to $\pm\delta$. Substituting (7) and the above-found value of θ into (5)₁, we find

$$\bar{\epsilon} = -\dot{\epsilon} \cos(2\chi \pm 2\delta). \quad (9)$$

Therefore, (9) is one of the necessary conditions for a plastic deformation to occur.

We shall show that we have now a set of sufficient conditions for a plastic deformation to occur. Equations (3), (4), (5) and (9) may be regarded as a parametric expression of the constitutive equations. Eliminating parameters θ , $\bar{\sigma}$, and $\bar{\epsilon}$, we can find explicit forms of the constitutive equations. The simplest is the following matrix expression:

$$\frac{\sigma}{\dot{\epsilon}} \begin{bmatrix} \dot{\epsilon}'_{xx} & \dot{\epsilon}'_{xy} \\ \dot{\epsilon}'_{xy} & \dot{\epsilon}'_{yy} \end{bmatrix} = \begin{bmatrix} \cos 2\chi & -\sin 2\chi \\ \sin 2\chi & \cos 2\chi \end{bmatrix} \begin{bmatrix} \sigma'_x & \tau_{xy} \\ \tau_{xy} & \sigma'_y \end{bmatrix} \quad (10)$$

where a prime signifies that the respective quantity is deviatoric. This equation shows that λ in (8) is given by $\hat{\epsilon}/\hat{\sigma}$. If the deviators $\epsilon'_{ij} = \epsilon_{ij} - \bar{\epsilon}$ and $\sigma'_{ij} = \sigma_{ij} - \bar{\sigma}$ are relegated to restore the regular components ϵ_{ij} and σ_{ij} , we find, as shown in ref. 20, that (10) yields the most general form (8). Note that the constitutive equations thus derived contain χ .

Equation (9) is as significant to the strain-rate tensor as the Coulomb criterion (4) is to the stress tensor, and is called the *volume characteristic*. The rate of volume change

$$\bar{\epsilon} = -\frac{1}{2} \left(\frac{\partial v_x}{\partial x} + \frac{\partial v_y}{\partial y} \right) \quad (11)$$

can be positive, zero, or negative depending on the value of non-coaxial angle χ . The volume characteristic was derived in ref. 20 without assuming (8), but the use of the theory of characteristic lines in this paper is much more elemental than in ref. 20. It was shown in ref. 20 that the theory of plastic potential does or does not apply when either $\chi = 0$ or $\neq 0$, respectively.

Density γ can be determined by use of $\bar{\epsilon}$: the equation of the conservation of mass

$$\frac{\partial \gamma}{\partial t} + \text{div}(\gamma \mathbf{v}) = 0$$

yields

$$\frac{\partial \gamma}{\partial t} + \nu \frac{\partial \gamma}{\partial s} = 2\bar{\epsilon}\gamma \quad (12)$$

where \mathbf{v} is the velocity vector, ν the velocity magnitude, and s the length of the flow line.

Strain-rate characteristic directions

We shall write out the $\dot{\epsilon}$ -singlet direction which is still not formulated. Eliminating the two parameters $\bar{\epsilon}$ and $\hat{\epsilon}$ from the three equations in (5), we find

$$A \frac{\partial v_x}{\partial x} - B \frac{\partial v_x}{\partial y} - B \frac{\partial v_y}{\partial x} - A \frac{\partial v_y}{\partial y} = 0 \quad (13)$$

where

$$A = \sin(2\theta + 2\chi)$$

$$B = \cos(2\theta + 2\chi).$$

We rewrite (9) to

$$A \frac{\partial v_x}{\partial x} + C \frac{\partial v_x}{\partial y} + C \frac{\partial v_y}{\partial x} + A \frac{\partial v_y}{\partial y} = 0 \quad (14)$$

where

$$C = \cos(2\chi \pm 2\delta)$$

by replacing $\bar{\epsilon}$ with (14) and eliminating $\hat{\epsilon}$ by use of (5)₃. Two uniqueness conditions

$$dv_x = \frac{\partial v_x}{\partial x} dx + \frac{\partial v_x}{\partial y} dy \quad (15)$$

$$dv_y = \frac{\partial v_y}{\partial x} dx + \frac{\partial v_y}{\partial y} dy \quad (16)$$

must also be satisfied.

Regard equations (13), (14), (15), and (16) as the simultaneous linear equations with four unknowns: $\partial v_x/\partial x$, $\partial v_y/\partial x$, $\partial v_x/\partial y$, and $\partial v_y/\partial y$. We can determine the characteristic directions by letting the denominator determinant equal zero (Courant and Hilbert,³ Abbott¹)

$$\begin{vmatrix} A & -B & -B & -A \\ A & C & C & A \\ dx & dy & 0 & 0 \\ 0 & 0 & dx & dy \end{vmatrix} = 0. \quad (17)$$

The quadratic equation (17) has two roots: one is (2), the doublet; the other is the $\dot{\epsilon}$ -singlet

$$\frac{dy}{dx} = \tan(\theta + 2\chi \pm \delta). \quad (18)$$

Equation (17) is the denominator of the solutions of the simultaneous linear equations (13), (14), (15), and (16) for the unknowns $\partial v_x/\partial x$, $\partial v_x/\partial y$, $\partial v_y/\partial x$, and $\partial v_y/\partial y$. Then, the numerators of the rational expressions of these unknowns must also be equal to zero. We can show that all four numerators reduce to a single equation

$$dv_x dx + dv_y dy = 0 \quad (19)$$

where dy/dx is either (2) or (18).

If we simply want to verify (19), it is much simpler to form a linear combination of (13) and (14). We can find that both (13) $\times \cos(2\theta \mp 2\delta)$ + (14) and (13) $\times \cos(2\theta + 4\chi \pm 2\delta)$ + (14) reduce to the same formula

$$\frac{\partial v_x}{\partial x} (dx)^2 + \left(\frac{\partial v_x}{\partial y} + \frac{\partial v_y}{\partial x} \right) dx dy + \frac{\partial v_y}{\partial y} (dy)^2 = 0 \quad (20)$$

where dy/dx is either (2) or (18). Equation (20) reduces to (19) by use of (15) and (16). Equation (20) is equivalent to

$$\dot{\epsilon}_{xx} (dx)^2 + 2\dot{\epsilon}_{xy} dx dy + \dot{\epsilon}_{yy} (dy)^2 = 0. \quad (21)$$

Therefore (19) means that the strain-rate characteristic lines neither elongate nor shrink.

Constitutive geometry

It is possible to express the constitutive relationships with the geometry of the $+m$ and $-m$ coincidences, as shown in Figures 4a and 4b, respectively.

In Figures 4a and 4b, $+m$ and $-m$ doublets are at D and E, $+m$ and $-m$ σ -singlets are at E_σ and D_σ , and $+m$ and $-m$ $\dot{\epsilon}$ -singlets are at E_ϵ and D_ϵ , respectively. Equations (2) and (18) give, as shown at P, the angles that σ - and $\dot{\epsilon}$ -characteristic directions make with the x -axis. Point O'_ϵ is the intersection of the two tangents drawn at the strain-rate characteristic points. Details of the geometric relationship are described in the following.

Proposition 1. The $\dot{\epsilon}$ -singlet direction makes angle $2\chi \pm 2\delta$ with the doublet direction.

Proof. Compare the arguments of the tangent functions in (18) and (2).

Proposition 2. The $\dot{\epsilon}$ -singlet is by the central angle 4χ apart from the σ -singlet.

Proof. In the case of Figure 4a, note that

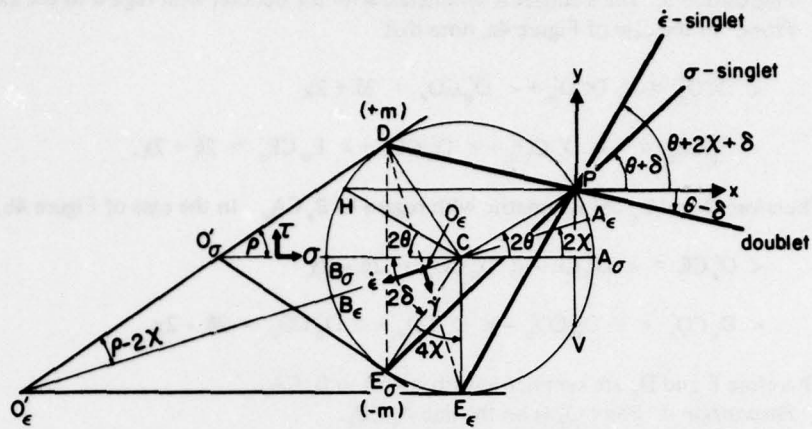


Figure 4a. Geometry of the +m coincidence.

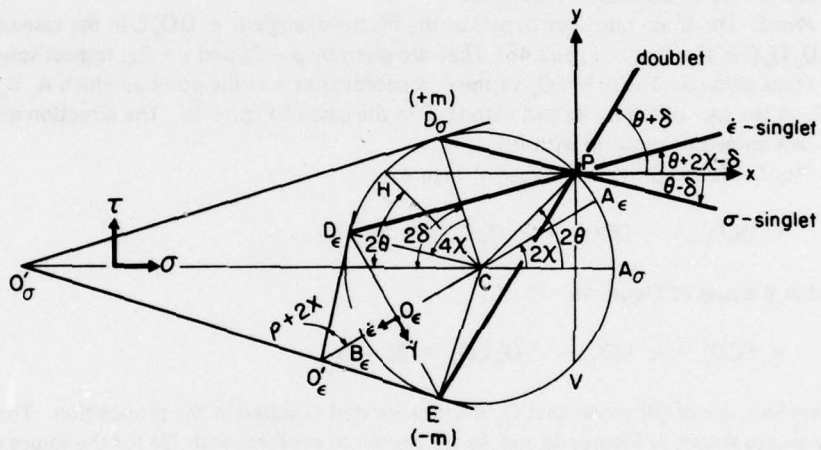


Figure 4b. Geometry of the -m coincidence.

$$\angle HCE_\epsilon = 2 \angle HPE_\epsilon = 2(\theta + 2X + \delta)$$

$$\angle HCE_\sigma = 2 \angle HPE_\sigma = 2(\theta + \delta).$$

Therefore

$$\angle E_\sigma CE_\epsilon = 4X.$$

In the case of Figure 4b, note that

$$\angle HCD_\epsilon = 2 \angle HPD_\epsilon = 2(\theta + 2X - \delta)$$

$$\angle D_\sigma CH = 2 \angle D_\sigma PH = -2(\theta - \delta).$$

Therefore

$$\angle D_\sigma CD_\epsilon = 4X.$$

Proposition 3. The $\dot{\epsilon}$ -singlet is symmetric with the doublet with regard to the axis $A_\epsilon B_\epsilon$.

Proof. In the case of Figure 4a, note that

$$\angle DCO'_\epsilon = \angle DCO'_\sigma + \angle O'_\sigma CO'_\epsilon = 2\delta + 2\chi$$

$$\angle O'_\epsilon CE_\epsilon = -\angle O'_\sigma CO'_\epsilon + \angle O'_\sigma CE_\sigma + \angle E_\sigma CE_\epsilon = 2\delta + 2\chi.$$

Therefore D and E_ϵ are symmetric with regard to $B_\epsilon CA_\epsilon$. In the case of Figure 4b, note that

$$\angle O'_\epsilon CE = \angle O'_\sigma CE - \angle O'_\sigma CO'_\epsilon = 2\delta - 2\chi$$

$$\angle D_\epsilon CO'_\epsilon = \angle D_\sigma CO'_\sigma - \angle D_\sigma CD_\epsilon + \angle O'_\sigma CO'_\epsilon = 2\delta - 2\chi.$$

Therefore E and D_ϵ are symmetric with regard to $B_\epsilon CA_\epsilon$.

Proposition 4. Point O'_ϵ is on the line $A_\epsilon CB_\epsilon$.

Proof. This is a corollary of Proposition 3.

Proposition 5. The strain rate counterpart of the frictional angle is $\rho - 2\chi$ in the case of Figure 4a and $\rho + 2\chi$ in the case of Figure 4b.

Proof. The strain rate counterpart of the frictional angle is $\angle DO'_\epsilon C$ in the case of Figure 4a and $\angle D_\epsilon O'_\epsilon C$ in the case of Figure 4b. They are given by $\rho - 2\chi$ and $\rho + 2\chi$, respectively.

Proposition 6. The origin O_ϵ of the $\dot{\epsilon}$, $\dot{\gamma}$ coordinates is at the point at which $A_\epsilon B_\epsilon$ intersects with DE_ϵ in the case of Figure 4a and with $D_\epsilon E$ in the case of Figure 4b. The direction of the $\bar{\epsilon}$ -axis must be determined to conform with (9).

Proof. We can prove in the case of Figure 4a

$$\angle DCO'_\epsilon = \angle DCO'_\sigma + \angle O'_\sigma CO'_\epsilon = 2\chi + 2\delta$$

and in the case of Figure 4b

$$\angle ECO'_\epsilon = \angle ECO'_\sigma - \angle O'_\sigma CO'_\epsilon = 2\delta - 2\chi.$$

Therefore, use of (9) shows that O_ϵ must be located as stated in the proposition. The directions of the $\bar{\epsilon}$ -axes shown in Figures 4a and 4b are chosen to conform with (9) for the values of 2χ as shown in these figures. Note that the negative and positive values of $\bar{\epsilon}$ are defined in this paper as dilation and contraction, respectively.

Proposition 7. In the case of $+m$ coincidence, $\bar{\epsilon}$ is positive or negative when A_ϵ in Figure 5a is on the arcs MDN or $ME_\sigma N$, respectively. In the case of $-m$ coincidence, $\bar{\epsilon}$ is positive or negative when A_ϵ in Figure 5b is on the arcs MEN or $MD_\sigma N$, respectively. Line MCN in Figure 5a or 5b is drawn parallel to $O'_\sigma D$ or $O'_\sigma E$, respectively.

Proof. Use of propositions 6 and 3 shows that, when A is at M, C is the origin of the $\dot{\epsilon}$, $\dot{\gamma}$ coordinates. On which side of MN point A_ϵ must be located to make $\dot{\epsilon} > 0$ or < 0 can be found by use of proposition 6 or (9).

STRAIN-RATE TENSOR

The dyadic expression

The relationships of the strain rate components in (5) and (9) give, as shown below, a simplified expression of strain rate tensor, which facilitates the transformation of curvilinear coordinates. To show this, second-order tensors must be expressed as dyadics (Wilson,²⁷ Brand,² Sedov,¹⁶ Yoshimura,²⁸ Takagi²²).

Letting the x - and y -directions be c_x and c_y , respectively, the strain rate tensor $\dot{\mathbf{E}}$ may be expressed as

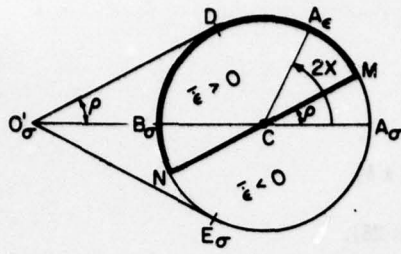


Figure 5a. Domains $\bar{\epsilon} \gtrless 0$ on the Mohr circle. The case of $+m$ coincidence is shown.

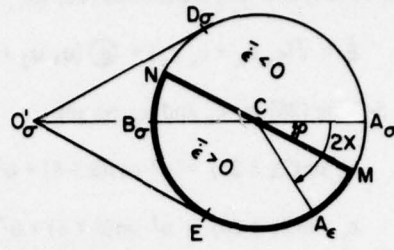


Figure 5b. Domains $\bar{\epsilon} \gtrless 0$ on the Mohr circle. The case of $-m$ coincidence is shown.

$$\dot{\epsilon} = \dot{\epsilon}_{xx} c_x c_x + \dot{\epsilon}_{xy} (c_x c_y + c_y c_x) + \dot{\epsilon}_{yy} c_y c_y. \quad (22)$$

The bases $c_x c_x$, $c_x c_y$, $c_y c_y$, and $c_y c_x$ of this tensor are dyads (Wilson,²⁷ Brand²). (Note that $c_x c_y \neq c_y c_x$; i.e., vectors are not commutative in a dyadic product.) In the conventional tensor analysis, tensor bases being omitted, the components are transformed; however, use of invariants $\bar{\epsilon}$ and $\dot{\epsilon}$ forces us to transform tensor bases. Substituting (5), we transform (22) to

$$\begin{aligned} \dot{\epsilon} = & \bar{\epsilon} (c_x c_x + c_y c_y) + \\ & + \dot{\epsilon} \left\{ [c_x \cos(\theta \mp \delta) + c_y \sin(\theta \mp \delta)] [c_x \cos(\theta + 2\chi \pm \delta) + c_y \sin(\theta + 2\chi \pm \delta)] - \right. \\ & \left. - [c_x \sin(\theta \mp \delta) - c_y \cos(\theta \mp \delta)] [c_x \sin(\theta + 2\chi \pm \delta) - c_y \cos(\theta + 2\chi \pm \delta)] \right\}. \end{aligned} \quad (23)$$

This will further be transformed in the following to a compact dyadic expression.

Case 1. When $2\chi \pm 2\delta \neq n\pi$ (n is an integer), the doublet (2) and the $\dot{\epsilon}$ -singlet (18) are distinct. We denote the directions of the doublet and the $\dot{\epsilon}$ -singlet by the *subscripted* unit base vectors u_1 and u_2 , respectively,

$$\begin{aligned} u_1 &= c_x \cos(\theta \mp \delta) + c_y \sin(\theta \mp \delta) \\ u_2 &= c_x \cos(\theta + 2\chi \pm \delta) + c_y \sin(\theta + 2\chi \pm \delta). \end{aligned} \quad (24)$$

When $2\chi \pm 2\delta \neq 0$, vectors u_1 and u_2 are not orthogonal; then it is convenient to introduce *superscripted* vectors e^1 and e^2 defined by $e^i \cdot u_j = \delta_j^i$, where δ_j^i is a Kronecker delta, and $a \cdot b$ means the dot (scalar) product of vectors a and b . It is more convenient in this case to use the directions u^1 and u^2 of e^1 and e^2 , respectively, instead of e^1 and e^2 themselves; in more detail, components, if appropriately chosen, of a tensor expressed with dual unit vectors u_i , u^i ($i = 1, 2$) can mean *physical components*, i.e., components with clear physical meaning. We determine the senses, which are still left undecided, of the superscripted unit base vectors u^1 , u^2 by making them satisfy

$$u_1 \cdot u^1 = u_2 \cdot u^2. \quad (25)$$

Thus, the two vectors are determined:

$$\begin{aligned} u^1 &= c_x \sin(\theta + 2\chi \pm \delta) - c_y \cos(\theta + 2\chi \pm \delta) \\ u^2 &= -c_x \sin(\theta \mp \delta) + c_y \cos(\theta \mp \delta). \end{aligned} \quad (26)$$

Use of (24) and (26) transforms (23) to

$$\dot{\mathbf{E}} = \bar{\mathbf{e}}(c_x c_x + c_y c_y) + \mathbf{\hat{e}}(u_1 u_2 + u^2 u^1). \quad (27)$$

Solving (26) for c_x and c_y , we get

$$c_x \sin(2\chi \pm 2\delta) = u^1 \cos(\theta \mp \delta) + u^2 \cos(\theta + 2\chi \pm \delta) \quad (28)$$

$$c_y \sin(2\chi \pm 2\delta) = u^1 \sin(\theta \mp \delta) + u^2 \sin(\theta + 2\chi \pm 2\delta).$$

Substituting (28) into (24), we get

$$u_1 \sin(2\chi \pm 2\delta) = u^1 + u^2 \cos(2\chi \pm 2\delta)$$

$$u_2 \sin(2\chi \pm 2\delta) = u^1 \cos(2\chi \pm 2\delta) + u^2.$$

By use of the formulas derived above, we can transform all the base vectors in $\dot{\mathbf{E}}$ in (27) to u^1 and u^2 ; then, $\dot{\mathbf{E}}$ should take the form

$$\dot{\mathbf{E}} = \dot{\epsilon}_{11} u^1 u^1 + \dot{\epsilon}_{12} (u^1 u^2 + u^2 u^1) + \dot{\epsilon}_{22} u^2 u^2. \quad (29)$$

Actual calculation yields that

$$\dot{\epsilon}_{11} = 0$$

$$\dot{\epsilon}_{22} = 0 \quad (30)$$

$$\dot{\epsilon}_{12} = \mathbf{\hat{e}}.$$

The actual calculation shows that $(30)_1$ and $(30)_2$ are the two equations in (19), as shown by (21).

Vector u^i defined by the convention (25) does not necessarily make an acute angle with u_i , as in the case of the orthodox definition $e^i \cdot e_j = \delta^i_j$. However, the angles between u_i and u^j are simultaneously either acute or obtuse; then, dyads in (29) do not change sign; therefore, the components do not change sign. Thus, the convention (25) completely serves our purpose. Finally, let us note that we prefer the new terminology of "subscripted" and "superscripted" to the classical terminology of "covariant" and "contravariant."

Case 2. When $2\chi \pm 2\delta = n\pi$, there is a single coincident $\dot{\epsilon}$ -characteristic direction; and the decomposition (23) does not work. In this case, (9) and (5) reduce to

$$\bar{\mathbf{e}} = (-1)^{n-1} \mathbf{\hat{e}}$$

$$\dot{\epsilon}_{xx} = (-1)^{n-1} 2 \mathbf{\hat{e}} \sin^2(\theta \mp \delta)$$

$$\dot{\epsilon}_{yy} = (-1)^{n-1} 2 \mathbf{\hat{e}} \cos^2(\theta \mp \delta)$$

$$\dot{\epsilon}_{xy} = (-1)^n \mathbf{\hat{e}} \sin(2\theta \mp 2\delta).$$

Then, (22) transforms to

$$\dot{\mathbf{E}} = (-1)^{n-1} 2 \mathbf{\hat{e}} [c_x \sin(\theta \mp \delta) - c_y \cos(\theta \mp \delta)] [c_x \sin(\theta \mp \delta) - c_y \cos(\theta \mp \delta)].$$

We will transform this to a compact dyadic expression.

Let u_1 and u_2 be the directions of the doublet and the σ -singlet, respectively,

$$u_1 = c_x \cos(\theta \mp \delta) + c_y \sin(\theta \mp \delta)$$

$$u_2 = c_x \cos(\theta \pm \delta) + c_y \sin(\theta \pm \delta).$$

Let u^1 and u^2 be the reciprocal directions

$$u^1 = c_x \sin(\theta \mp \delta) - c_y \cos(\theta \pm \delta)$$

$$u^2 = -c_x \sin(\theta \mp \delta) + c_y \cos(\theta \mp \delta)$$

satisfying the convention in (25). Then (31) becomes

$$\dot{\xi} = (-1)^{n-1} 2 \dot{\epsilon} u^2 u^2. \quad (32)$$

Therefore, components of $\dot{\xi}$ are given by

$$\dot{\xi}_{11} = 0$$

$$\dot{\xi}_{22} = (-1)^{n-1} 2 \dot{\epsilon} \quad (33)$$

$$\dot{\xi}_{12} = 0.$$

When $2\chi \pm 2\delta = n\pi$, (19) yields only one equation, $\dot{\xi}_{11} = 0$. The missing equation is supplied here; it is $\dot{\xi}_{12} = 0$.

Plastic work rate

The radius $\dot{\epsilon}$ is a factor of the plastic work rate. The plastic work rate \dot{W} is defined by

$$\dot{W} = \sigma_x \dot{\epsilon}_{xx} + 2\tau_{xy} \dot{\epsilon}_{xy} + \sigma_y \dot{\epsilon}_{yy}.$$

Substituting (3) and (5) and using (4) and (9), it becomes

$$\dot{W} = 2 \dot{\epsilon} \cot \rho [c \cos(2\chi \pm 2\delta) \pm \sigma \sin 2\chi]. \quad (34)$$

This quantity must be positive or zero, if no other irreversible process is concurrent. The condition

$$\dot{\epsilon} \geq 0 \quad (35)$$

must always be satisfied.

Coordinate transformation

Equations of motion are found by transforming either (19) or (33)₃. In addition we must formulate $\dot{\epsilon}$ to evaluate density γ by use of (12). In most cases, the coordinates of (19) can easily be transformed. However, formulation of $\dot{\xi}_{12}$ in (30)₂ and (33)₃, and $\dot{\xi}_{22}$ in (33)₂, in terms of velocity components needs elaborate transformation of the strain-rate tensor, as described below.

Because, in the following we must deal with the skew curvilinear coordinate system, we need a more expressive tensor notation than the conventional. We express the strain rate tensor $\dot{\xi}$ in the following invariant differential form. Letting x, y, c_x , and c_y be renamed ξ^1, ξ^2, e^1 , and e^2 , we rewrite $\dot{\xi}$, defined by (22), by use of (6), as

$$\dot{\mathbf{e}}^i = -\frac{1}{2} \left(\mathbf{e}^i \frac{\partial \mathbf{v}}{\partial \xi^j} + \frac{\partial \mathbf{v}}{\partial \xi^i} \mathbf{e}^j \right) \quad (36)$$

where i is the summation index and

$$\mathbf{v} = \nu_x \mathbf{c}_x + \nu_y \mathbf{c}_y. \quad (37)$$

The operator

$$\mathbf{e}^i \frac{\partial}{\partial \xi^i} = c_x \frac{\partial}{\partial x} + c_y \frac{\partial}{\partial y} \quad (38)$$

is an invariant, denoted by ∇ , or, as often called grad. Equation (36) is convenient for complicated coordinate transformation.

We define curvilinear coordinates ξ^1 and ξ^2 by

$$x = x(\xi^1, \xi^2) \quad (39)$$

$$y = y(\xi^1, \xi^2).$$

Curves ξ^1 and ξ^2 are such curves on which only ξ^1 and ξ^2 , respectively, vary and ξ^2 and ξ^1 are, respectively, kept constant. We define \mathbf{e}_1 and \mathbf{e}_2 by vectors tangent to curves ξ^1 and ξ^2 , respectively. Lengths of \mathbf{e}_1 and \mathbf{e}_2 must satisfy the relation

$$\begin{aligned} d\mathbf{r} &= c_x dx + c_y dy \\ &= \mathbf{e}_1 d\xi^1 + \mathbf{e}_2 d\xi^2. \end{aligned} \quad (40)$$

This equation gives \mathbf{e}_1 and \mathbf{e}_2 as follows:

$$\mathbf{e}_i = \frac{\partial \mathbf{r}}{\partial \xi^i} = c_x \frac{\partial x}{\partial \xi^i} + c_y \frac{\partial y}{\partial \xi^i}. \quad (41)$$

We then define reciprocal vectors \mathbf{e}^i by

$$\mathbf{e}^i \cdot \mathbf{e}_j = \delta_j^i. \quad (42)$$

We may reinterpret the operator $\mathbf{e}^i \partial / \partial \xi^i$ on the left-hand side of (38) in terms of the new definition. We can prove that (38) is still true even in the new definition. To prove this, note that \mathbf{e}^i may be written as

$$\mathbf{e}^i = c_x \frac{\partial \xi^i}{\partial x} + c_y \frac{\partial \xi^i}{\partial y} \quad (43)$$

because this expression satisfies (42). Substitution of (43) reduces the left-hand side of (38) to the right-hand side.

Note that the derivatives $\partial \mathbf{e}_i / \partial \xi^i$ and $\partial \mathbf{e}^i / \partial \xi^i$ can be calculated by use of (41) and (43), respectively, because c_x and c_y are constant. Therefore, even if \mathbf{v} may be expressed with bases \mathbf{e}_i or \mathbf{e}^i , the right-hand side of (36) can be reduced to the right-hand side of (29), where \mathbf{u}_i and \mathbf{u}^i are directions of \mathbf{e}_i and \mathbf{e}^i , respectively.

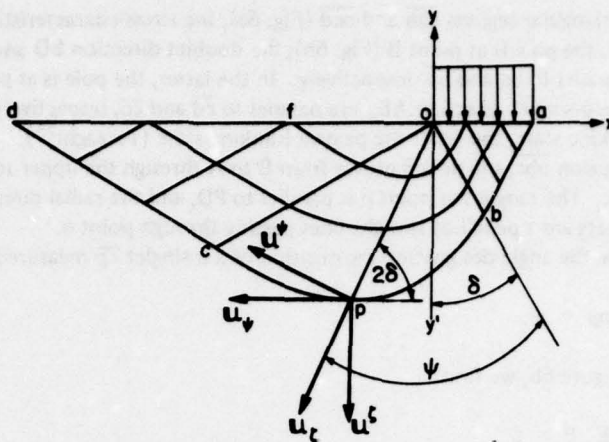


Figure 6a. A net of stress characteristic lines in the ground sustaining a rectangular load.

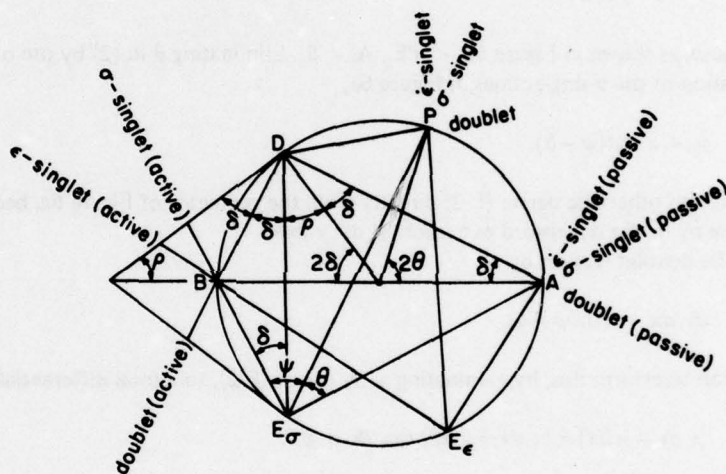


Figure 6b. Geometry of the characteristic directions of Figure 6a.

EXAMPLE

Figure 6a shows a net of stress characteristic lines caused in the ground sustaining a vertical rectangular load applied along the segment \overline{oa} on the horizontal ground surface. The line \overline{abpcd} is the slip line. Hill¹¹ gave the original solution, as explained by Prager and Hodge,¹⁵ for the case of frictional angle $\rho = 0$. Figure 6a is an extension of Hill's solution to the case of $\rho \neq 0$, as explained in the following. We shall fit the simplest velocity solution into the extended Hill's solution.

The stress solution

In terms of the geometry of the Mohr circle, the solution may be explained as follows:

In Figure 6a, the soil below the line \overline{abpcd} does not move and only the soil above \overline{abpcd} moves. We may assume that the tangential stress on the upper side of the line \overline{abpcd} is in the direction of the soil flow; then, the sign m on the line \overline{abpcd} is $+$. Therefore, the doublet is at point D in Figure 6b, and the σ -singlet is at E_σ .

In the triangular regions \overline{oab} and \overline{ocd} (Fig. 6a), the stress-characteristic lines are rectilinear. In the former, the pole is at point B (Fig. 6b); the doublet direction BD and the σ -singlet direction BE_σ are parallel to \overline{ba} and \overline{bo} , respectively. In the latter, the pole is at point A; the doublet direction AD and the σ -singlet direction AE_σ are parallel to \overline{cd} and \overline{co} , respectively. The former is called the active Rankine state, the latter the passive Rankine state (Terzaghi²⁴).

In the region \overline{obc} , the pole P moves from B to A through the upper semicircle, as point p moves from b to c. The tangent at point p is parallel to PD, and the radial direction \overline{op} is parallel to PE_σ . The σ -singlets are a pencil of straight lines passing through point o.

Let ψ be the angle designating the position of a σ -singlet \overline{op} measured from \overline{ob} in Figure 6a

$$\angle bop = \psi.$$

Then, in Figure 6b, we find

$$\angle BE_\sigma P = \psi.$$

Thus, we can prove that

$$\theta + \psi = \pi/2 \quad (E-1)$$

because, as shown in Figure 6b, $\angle PE_\sigma A = \theta$. Eliminating θ in (2) by use of (E-1), we get the equation of the σ -singlet lines in Figure 6a,

$$y = x \cot(\psi - \delta). \quad (E-2)$$

We can otherwise derive (E-2) directly from the geometry of Figure 6a, because $\angle boy' = \delta$, where oy' is the downward extension of the y-axis.

The doublet is given by

$$dy/dx = \cot(\psi + \delta). \quad (E-3)$$

We can transform this, by eliminating ψ by use of (E-2), to a total differential equation

$$(x dy - y dx) + (x dx + y dy) \tan 2\delta = 0.$$

To integrate this, let

$$\begin{aligned} x &= -r \sin(\psi - \delta) \\ y &= -r \cos(\psi - \delta) \end{aligned} \quad (E-4)$$

where r is the radial coordinate of a point under consideration. Then we get

$$r = \xi e^{\psi \tan \rho} \quad (E-5)$$

where ξ is the value of r at $\psi = 0$, i.e., on the initial line \overline{ob} .

Velocity equations in the σ -characteristic curvilinear coordinates

We shall fit a velocity field into the stress field obtained above. Because χ is unknown, we shall use the σ -characteristic curvilinear coordinates ξ, ψ . Because this curvilinear coordinate system is skew, we need a more general and simpler approach, i.e., use of base vectors, to introduce skew curvilinear analysis. Let the directions of curves ξ and ψ be u_ξ and u_ψ ,

$$u_{\zeta} = -c_x \sin(\psi - \delta) - c_y \cos(\psi - \delta) \quad (\text{E-6})$$

$$u_{\psi} = -c_x \sin(\psi + \delta) - c_y \cos(\psi + \delta). \quad (\text{E-7})$$

These equations are found by use of (2) with the substitution of θ from (E-1).

In addition to the subscripted base vectors u_{ζ} and u_{ψ} , we introduce the superscripted base vectors u^{ζ} and u^{ψ} . They are unit vectors defined by

$$u^{\zeta} \cdot u_{\psi} = 0$$

$$u^{\psi} \cdot u_{\zeta} = 0$$

$$u_{\zeta} \cdot u^{\zeta} = u_{\psi} \cdot u^{\psi} = \sin 2\delta.$$

They are given by

$$u^{\zeta} = c_x \cos(\psi + \delta) - c_y \sin(\psi + \delta) \quad (\text{E-8})$$

$$u^{\psi} = -c_x \cos(\psi - \delta) + c_y \sin(\psi - \delta). \quad (\text{E-9})$$

These four vectors are directed as shown in Figure 6a. The radial \overline{op} makes angle 2δ with the doublet at p , because $u_{\zeta} \cdot u_{\psi} = \cos 2\delta$.

We decompose velocity v into the directions u_{ψ} and u^{ζ} ,

$$v = v_1 u_{\psi} + v_2 u^{\zeta}. \quad (\text{E-10})$$

Note that u^{ζ} is normal to u_{ψ} . Substituting u_{ψ} from (E-7) and u^{ζ} from (E-8) into (E-10), and comparing the result with

$$v = v_x c_x + v_y c_y$$

we get

$$v_x = -v_1 \sin(\psi + \delta) + v_2 \cos(\psi + \delta) \quad (\text{E-11})$$

$$v_y = -v_1 \cos(\psi + \delta) - v_2 \sin(\psi + \delta).$$

Then, substituting v_x and v_y from (E-11) and dy/dx from (E-3), (19) in the case of the doublet direction transforms to

$$\frac{\partial v_1}{\partial s} + v_2 \frac{\partial \psi}{\partial s} = 0 \quad (\text{E-12})$$

where s is the length along a doublet curve. The \hat{e} -singlet is $+m$ coincident and is given from (18) by

$$dy/dx = \cot(\psi - 2\chi - \delta). \quad (\text{E-13})$$

Substituting v_x and v_y from (E-11) and dy/dx from (E-13), (19) in the case of the \hat{e} -singlet direction becomes

$$\cos(2\chi + 2\delta) \left(\frac{\partial v_1}{\partial t} + v_2 \frac{\partial \psi}{\partial t} \right) - \sin(2\chi + 2\delta) \left(\frac{\partial v_2}{\partial t} - v_1 \frac{\partial \psi}{\partial t} \right) = 0 \quad (\text{E-14})$$

where t is the length along the \hat{e} -singlet curve.

We shall express (E-12) and (E-14) with curvilinear coordinates ψ, ζ . Coordinates ψ and ζ are related to coordinates x, y and s, t by

$$dr = c_x dx + c_y dy \quad (E-15)$$

$$= e_\zeta d\zeta + e_\psi d\psi \quad (E-16)$$

$$= u_s ds + u_t dt \quad (E-17)$$

where u_s and u_t are directions of the doublet and the \hat{e} -singlet, respectively. We cannot use the \hat{e} -characteristic curvilinear coordinates in s - and t -directions, because χ is unknown.

We express x, y as functions of ζ and ψ by substituting (E-5) into (E-4), substitute these into (E-15), and compare the coefficients of $d\zeta$ and $d\psi$ in the transformed (E-15) and the untransformed (E-16); thus we find

$$e_\zeta = e^{\psi \tan \rho} u_\zeta \quad (E-18)$$

$$e_\psi = \frac{\zeta}{\sin 2\delta} e^{\psi \tan \rho} u_\psi.$$

It is obvious that

$$u_s = u_\zeta. \quad (E-19)$$

In the Cartesian coordinates, u_t is given by

$$u_t = -c_x \sin(\psi - 2\chi - \delta) - c_y \cos(\psi - 2\chi - \delta) \quad (E-20)$$

where (E-13) is used. We solve (E-6) and (E-7) for c_x and c_y , substitute these results into (E-20), and find

$$u_t \sin 2\delta = u_\zeta \sin(2\chi + 2\delta) - u_\psi \sin 2\chi. \quad (E-21)$$

We substitute (E-18) into (E-16), and (E-19) and (E-21) into (E-17), compare the coefficients of u_ζ and u_ψ in the two transformed equations, and find

$$e^{\psi \tan \rho} d\zeta = \frac{\sin(2\chi + 2\delta)}{\sin 2\delta} dt$$

$$\frac{\zeta}{\sin 2\delta} e^{\psi \tan \rho} d\psi = ds - \frac{\sin 2\chi}{\sin 2\delta} dt.$$

Use of the above equations yields

$$e^{\psi \tan \rho} \frac{\partial}{\partial s} = \frac{\sin 2\delta}{\zeta} \frac{\partial}{\partial \psi} \quad (E-22)$$

$$e^{\psi \tan \rho} \frac{\partial}{\partial t} = \frac{\sin(2\chi + 2\delta)}{\sin 2\delta} \frac{\partial}{\partial \zeta} - \frac{\sin 2\chi}{\zeta} \frac{\partial}{\partial \psi}.$$

Thus (E-12) becomes

$$\frac{\partial v_1}{\partial \psi} + v_2 = 0 \quad (E-23)$$

and (E-14) becomes

$$-\frac{1}{\sin 2\delta} \left[\frac{\partial v_1}{\partial \xi} \cos(2\chi + 2\delta) + \frac{\partial v_2}{\partial \xi} \sin(2\chi + 2\delta) \right] + \frac{\sin 2\chi}{\xi} \left(\frac{\partial v_2}{\partial \psi} - v_1 \right) = 0. \quad (\text{E-24})$$

The constant speed solution

We shall find the simplest velocity field that can be fitted in Figure 6a. If we denote by V the velocity on the segment \overline{oa} in the doublet direction \overline{ab} , the simplest solution in the rectilinear region \overline{oab} under the condition that \overline{oab} is the slip line is

$$v_1 = V \quad (\text{E-25})$$

$$v_2 = 0$$

where the decomposition of v into the doublet direction and the normal to the doublet direction as shown in (E-10) is still used. Equations (E-25) are the solution even in the curvilinear region \overline{obc} , if

$$\chi = 0 \quad (\text{E-26})$$

because (E-25) satisfies (E-23) and (E-24) on this assumption. We can find, if we will, more complicated solutions; however, in this paper, we are not interested in deriving them.

In the rectilinear regions \overline{oab} , the above solution gives $\hat{\epsilon} = 0$, and therefore $\dot{W} = 0$. However, this conclusion does not hold true in the curvilinear region \overline{obc} . To calculate $\hat{\epsilon}$ in this case, we shall compute $e^i (\partial v / \partial \xi^i)$ contained in (36), which, in this case, becomes

$$e^i \frac{\partial v}{\partial \xi^i} = e^\xi \frac{\partial v}{\partial \xi} + e^\psi \frac{\partial v}{\partial \psi}. \quad (\text{E-27})$$

The superscripted base vectors are determined by applying (E-18) to (42)

$$e^\xi = \frac{1}{\cos \rho} e^{-\psi \tan \rho} u^\xi \quad (\text{E-28})$$

$$e^\psi = \frac{1}{\xi} e^{-\psi \tan \rho} u^\psi.$$

To differentiate v in (E-10), note that (E-7) and (E-8) yield the following relations:

$$\frac{\partial u_\psi}{\partial \xi} = 0$$

$$\frac{\partial u_\psi}{\partial \psi} = -u^\xi$$

$$\frac{\partial u^\xi}{\partial \xi} = 0$$

$$\frac{\partial u^\xi}{\partial \psi} = u_\psi.$$

Thus (E-27) transforms to

$$\begin{aligned}
& e^{\psi} \tan \rho \cos \rho e^i \frac{\partial v}{\partial \xi^i} \\
&= \frac{\partial v_1}{\partial \xi} u^s u_\psi + \frac{\partial v_2}{\partial \xi} u^s u^s + \frac{\sin 2\delta}{\xi} \left(\frac{\partial v_1}{\partial \psi} + v_2 \right) u^\psi u_\psi + \frac{\sin 2\delta}{\xi} \left(\frac{\partial v_2}{\partial \psi} - v_1 \right) u^\psi u^s \quad (E-29)
\end{aligned}$$

where we have used (E-28) to change e^s and e^ψ to u^s and u^ψ , respectively.

We shall transform (E-29) to the form of (29); i.e., we shall change the base vectors in (E-29) to u^s and u^t , where u_s and u_t are given by (E-19) and (E-20), respectively. We find

$$u^s = -c_x \cos(\psi - 2\chi - \delta) + c_y \sin(\psi - 2\chi - \delta)$$

$$u^t = c_x \cos(\psi + \delta) - c_y \sin(\psi + \delta)$$

where the condition (25) is observed. Solving the above two equations for c_x and c_y , and substituting this solution into (E-7), (E-8), and (E-9), we can express u_ψ , u^s , and u^ψ in terms of u^s and u^t . Substituting these results into (E-29), we find

$$\begin{aligned}
& e^{\psi} \tan \rho \cos \rho \left(e^i \frac{\partial v}{\partial \xi^i} \right) \sin^2(2\chi + 2\delta) \\
&= \frac{\partial v_1}{\partial \xi} u^t \sin(2\chi + 2\delta) [u^s + u^t \cos(2\chi + 2\delta)] + \\
&+ \frac{\partial v_2}{\partial \xi} u^t u^t \sin^2(2\chi + 2\delta) + \\
&+ \frac{\sin 2\delta}{\xi} \left(\frac{\partial v_1}{\partial \psi} + v_2 \right) [u^s \sin 2\delta - u^t \sin 2\chi] [u^s + u^t \cos(2\chi + 2\delta)] + \\
&+ \frac{\sin 2\delta}{\xi} \left(\frac{\partial v_2}{\partial \psi} - v_1 \right) [u^s \sin 2\delta - u^t \sin 2\chi] u^t \sin(2\chi + 2\delta). \quad (E-30)
\end{aligned}$$

Changing the order of base vectors in the dyadic products in (E-30), we construct the right-hand side of (36); then, we can determine coefficients $\hat{\epsilon}_{11}$, $\hat{\epsilon}_{22}$, and $\hat{\epsilon}_{12}$ in (29). Thus, from the expression of $\hat{\epsilon}_{12}$, we find

$$\hat{\epsilon}_{12} = \frac{1}{2} e^{-\psi} \tan \rho \operatorname{cosec}(2\chi + 2\delta) \left\{ -\frac{\partial v_1}{\partial \xi} + \frac{\sin^2 2\delta}{\xi} \left(v_1 - \frac{\partial v_2}{\partial \psi} \right) \right\}.$$

The expressions of the components $\hat{\epsilon}_{11}$ and $\hat{\epsilon}_{22}$ give equations (E-23) and (E-24), respectively. Therefore, in the simplest solution (E-25), $\hat{\epsilon}$ is given by

$$\hat{\epsilon} = \frac{1}{2} V \cos \rho \frac{1}{\xi} e^{-\psi} \tan \rho. \quad (E-31)$$

To determine the variation of density γ under the steady condition

$$\frac{\partial \gamma}{\partial t} = 0$$

note that the use of (E-22) enables us to change $\partial/\partial s$ to $\partial/\partial \psi$; we evaluate $\bar{\epsilon}$ in (9) by use of (E-26) and (E-31); then, (12) yields

$$\frac{1}{\gamma} \frac{\partial \gamma}{\partial \psi} = -\tan \rho.$$

Therefore, if the density in the active region oab (Fig. 6a) is constant, denoted by γ_0 , the dilatation occurs as described by the equation

$$\gamma = \gamma_0 e^{-\psi \tan \rho}.$$

If the dilatation continues at the rate given by this equation, the density γ_p in the passive region must be

$$\gamma_p = \gamma_0 e^{-(\pi/2) \tan \rho}. \quad (\text{E-32})$$

If $\rho = 30^\circ$, this equation gives $\gamma_p/\gamma_0 = 0.402$. If the dilatation is too large, the minimum density γ_1 must be reached at angle ψ_0 ,

$$\gamma_1 = \gamma_0 e^{-\psi_0 \tan \rho} \quad (\text{E-33})$$

and maintained in the region $\psi \geq \psi_0$.

Point 0 is a singular point, at which (E-31) yields

$$\bar{\epsilon} = \infty.$$

We cannot yet discuss the mathematical modification necessitated by the physical impossibility of the singularity at point 0.

Velocity equations in the constant density region

If the flow is steady and $\bar{\epsilon} = 0$, density γ is constant, as (12) shows us, along the flow lines. Therefore, χ in the $+m$ -coincident constant density region must be given by

$$\chi = \rho/2 \quad (\text{E-34})$$

where (9) is used. Therefore, the $\bar{\epsilon}$ -characteristic curves in this case are orthogonal.

The $+m$ -coincident $\bar{\epsilon}$ -singlets are given by

$$\frac{dy}{dx} = \cot(\psi - \rho - \delta)$$

where (18), (E-1), and (E-34) are used. Eliminating ψ by use of (E-2), this equation becomes a total differential equation

$$(y dx - x dy) + (x dx + y dy) \tan \rho = 0.$$

This integrates to

$$r = \eta e^{-(\psi - \psi_0) \cot \rho}$$

by use of (E-4), where η is the initial value of r in the constant-density region. In this case we express the doublet in (E-5) with

$$r = \xi e^{(\psi - \psi_0) \tan \rho}$$

where ξ is the value of r at $\psi = \psi_0$. Solving the above two equations we find

$$\psi - \psi_0 = \lambda \log(\eta/\xi) \quad (\text{E-35})$$

where

$$\lambda = \sin \rho \cos \rho.$$

We introduce the curvilinear coordinates ξ and η in place of the lengths s and t of the doublet and the ϵ -singlet, respectively. We transform (E-12) and (E-14) to

$$\frac{\partial v_1}{\partial \eta} + v_2 \frac{\partial \psi}{\partial \eta} = 0$$

$$\frac{\partial v_2}{\partial \xi} - v_1 \frac{\partial \psi}{\partial \xi} = 0$$

where (E-34) is used. These equations reduce to

$$\frac{\partial v_1}{\partial y} + v_2 = 0 \quad (\text{E-36})$$

$$\frac{\partial v_2}{\partial x} + v_1 = 0 \quad (\text{E-37})$$

when we put

$$x = \lambda \log \xi \quad (\text{E-38})$$

$$y = \lambda \log \eta.$$

Thus, we find that v_1 and v_2 are governed by the equations

$$\frac{\partial^2 v_1}{\partial x \partial y} = v_1 \quad (\text{E-39})$$

$$\frac{\partial^2 v_2}{\partial x \partial y} = v_2. \quad (\text{E-40})$$

These are the same types of hyperbolic differential equations whose boundary-value problems are completely solved (Courant and Hilbert,³ p. 458).

Solution in the first constant-density subregion

Let the line \overline{of} in Figure 7 be the initial line at which the constant density region begins. Draw the ϵ -singlet passing through f ; and let g be the intersection of the ϵ -singlet with the line \overline{oc} . The velocity and its derivatives must be continuous across \overline{of} , because this line is noncharacteristic in the velocity field. The unique solution of (E-39) must be found by use of the boundary conditions

$$v_1 = V, \quad \frac{\partial v_1}{\partial x} = 0, \quad \text{and} \quad \frac{\partial v_1}{\partial y} = 0$$

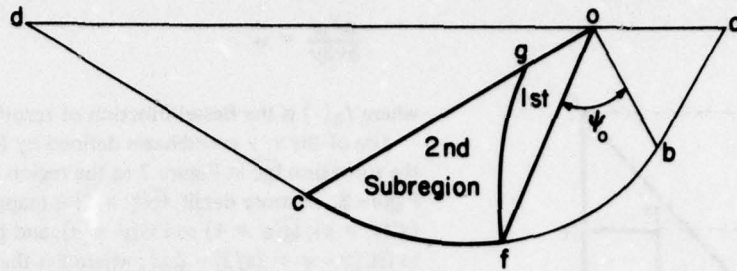


Figure 7. The first and second subregions of the constant density region.

on \overline{of} , where $\psi = \psi_0$, i.e., $x = y$.

Assume the solution

$$v_1 = F(t)$$

where

$$t = y - x.$$

Then (E-39) becomes

$$\frac{d^2 F}{dt^2} + F = 0.$$

Thus we find the solution

$$v_1 = V \cos(y - x).$$

Use of (E-36) yields

$$v_2 = V \sin(y - x).$$

Use of (E-38) and (E-35) transforms them to

$$v_1 = V \cos(\psi - \psi_0).$$

$$v_2 = V \sin(\psi - \psi_0).$$

Thus, the velocity vector \mathbf{v} is given by

$$\mathbf{v} = V[-c_x \sin(\psi_0 + \delta) - c_y \cos(\psi_0 + \delta)]$$

where (E-10), (E-7), and (E-8) are used. The direction of \mathbf{v} , therefore, is u_ψ evaluated at $\psi = \psi_0$. Therefore, the velocity in the region \overline{ofg} is constant, being equal to the initial velocity on the line \overline{of} .

Solution in the second constant density subregion

The solution in the subregion \overline{fgc} needs the use of the Riemann function

$$w(x, y) = J_0 [2\sqrt{(x-p)(q-y)}] \quad (\text{E-41})$$

which satisfies

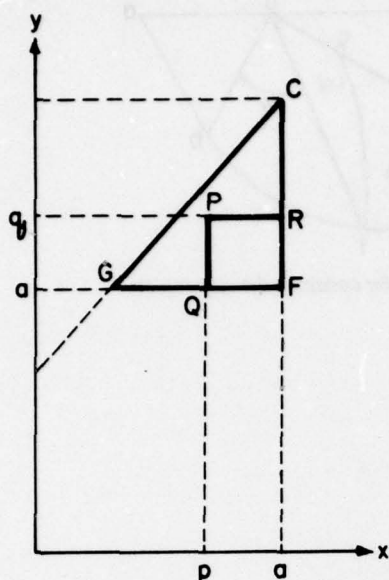


Figure 8. Solution in the second sub-region.

$$\frac{\partial^2 w}{\partial x \partial y} = w$$

where $J_0(\)$ is the Bessel function of zeroth order.

Use of the x, y coordinates defined by (E-38) maps the subregion $\bar{f}g\bar{c}$ in Figure 7 to the region FGC in Figure 8. In more detail, $\bar{f}c(\xi = \ell)$ is mapped to $FC(x = a)$; $\bar{f}g(\eta = \ell)$ to $FG(y = a)$; and $\bar{g}c[\psi = (\pi/2)]$ to $GC[y - x = (\pi/2) - \psi_0]$, where ℓ is the length of \bar{of} and $a = \lambda \log \ell$. In the following, we shall solve (E-39) on the assumption that v_1 and its normal derivative across the characteristic boundary $\bar{f}g$ are continuous. This assumption holds true for the normal component v_1 but does not for the tangential component v_2 on the characteristic boundary $\bar{f}g$.

Riemann's method in this case consists in the transformation of the identity

$$\iint_{\square PQRf} \left\{ w \frac{\partial^2 v_1}{\partial x \partial y} - v_1 \frac{\partial^2 w}{\partial x \partial y} \right\} dx dy = 0$$

where the range of integration is the rectangle PQRf in Figure 8. Point P is an arbitrary point with coordinates

(p, q) , and PQ and PR are parallel to y - and x -axes, respectively. The above equation transforms to

$$\iint_{\square PQRf} \left\{ \frac{\partial}{\partial y} \left(w \frac{\partial v_1}{\partial x} \right) - \frac{\partial}{\partial x} \left(v_1 \frac{\partial w}{\partial y} \right) \right\} dx dy = 0$$

which, on integration, becomes

$$\int_p^a \left\{ \left(w \frac{\partial v_1}{\partial x} \right)_{y=q} - \left(w \frac{\partial v_1}{\partial x} \right)_{y=a} \right\} dx - \int_a^q \left\{ \left(v_1 \frac{\partial w}{\partial y} \right)_{x=a} - \left(v_1 \frac{\partial w}{\partial y} \right)_{x=p} \right\} dy = 0.$$

Because

$$w(x, q) = 1, \quad v_1(a, y) = V, \quad \text{and} \quad \frac{\partial w}{\partial y}(p, y) = 0$$

we can integrate once more to find

$$v_1(p, q) = Vw(a, a) - \int_p^a w(x, a) \frac{\partial v_1}{\partial x}(x, a) dx$$

where $(\partial w / \partial y)(p, y)$ and $(\partial v_1 / \partial x)(x, a)$ are the notations meaning to let $x = p$ and $y = a$ in $(\partial / \partial y)w(x, y)$ and $(\partial / \partial x)v_1(x, y)$, respectively. Changing the dummy variables, we find the solution

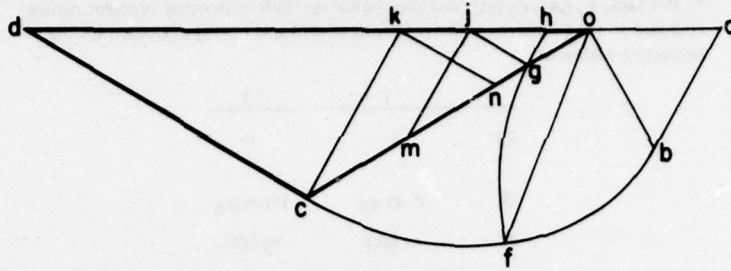


Figure 9. Velocity field in the passive region.

$$\frac{1}{V} v_1(x, y) = J_0[2\sqrt{(a-x)(y-a)}] - \int_x^a \sin(a-t) J_0[2\sqrt{(t-x)(y-a)}] dt. \quad (E-42)$$

Use of (E-36) yields

$$\begin{aligned} \frac{1}{V} v_2(x, y) = & \sqrt{\frac{a-x}{y-a}} J_1[2\sqrt{(a-x)(y-a)}] - \\ & - \frac{1}{\sqrt{y-a}} \int_x^a \sqrt{t-x} \sin(a-t) J_1[2\sqrt{(t-x)(y-a)}] dt. \end{aligned} \quad (E-43)$$

The boundary condition $v_2 \approx 0$ on \overline{fc} is satisfied. One can prove that v_2 is continuous on \overline{fg} but the normal derivative $\partial v_2 / \partial x$ is not.

Solution in the passive region

The density on a moving radial decreases as it moves from \overline{ob} to \overline{oc} in Figure 9. If γ_p in (E-32) is larger or equal to γ_1 , γ_p is actually reached and the constant-density region disappears. In this case, the velocity in the passive region \overline{ocd} is the simplest solution (E-25), where v_1 and v_2 are the velocity components along the doublet direction and the normal to the doublet direction, respectively.

If the minimum density γ_1 is larger than γ_p in (E-32), γ_1 is reached, say at \overline{of} in Figure 9, and γ_p cannot be reached, then, the velocity in the passive region becomes complicated, as explained in the following.

In the passive region, the doublets and the ϵ -singlets are straight lines; and velocity components along these lines are constant. Therefore, $\epsilon = 0$ in this case; and we have no means of determining χ . However, for the sake of presentation, we just assume $\chi = \rho/2$ and describe the following velocity field.

The velocity field in the passive region is determined by the velocity components on the boundaries \overline{oc} and \overline{cd} (Fig. 9). It is divided into various segments. We draw the doublet straight lines and the ϵ -singlet straight lines (orthogonal to the former) at the point g , and denote their intersections with \overline{od} by points j and h , respectively. We draw \overline{ck} and \overline{jm} parallel to the ϵ -singlet, and denote their intersections with \overline{od} and \overline{oc} by points k and m , respectively. Finally, we draw \overline{kn} parallel to the doublet and denote the intersection with \overline{oc} by point n . The velocity components on \overline{oc} , \overline{cd} , and \overline{od} are shown in Table I.

Table I. Velocity components on the boundaries of the passive region.
 In this table v_1 (gc), v_2 (gc), and the similar symbols with other segment names enclosed in the brackets are the solutions (E-42) and (E-43) evaluated on the respective segments.

	v_1	v_2
\bar{cd}	V	0
\bar{og}	$V \sin \psi_0$	$V \cos \psi_0$
\bar{gc}	v_1 (gc)	v_2 (gc)
\bar{oh}	$V \sin \psi_0$	$V \cos \psi_0$
\bar{hj}	$V \sin \psi_0$	v_2 (gm)
\bar{jk}	v_1 (gn)	v_2 (mc)
\bar{kd}	v_1 (nc)	0

CONCLUSION

The exposition in this paper reveals that the formulation of the in-plane deformation of the non-coaxial Coulomb material has reached the stage of completion. However, it is disclosed that the assignment of a set of boundary conditions cannot lead us to the unique determination of the non-coaxial angle; in addition, the mode of flow must be given to determine the non-coaxial angle uniquely.

We can propose several courses of further improvement, as explained below, that may remedy this defect. However, the non-coaxial angle is contained in the constitutive equations at any stage of the proposed improvement; therefore, *the constitutive equations of the Coulomb material are more than material constant*, even in the final satisfactory, if possible, formulation.

Two courses suggested by the rational mechanics formulation are looming in our prospective research area. The first is the introduction of couple stress. Mandl and Luque¹³ interpret the non-coaxial angle to be induced by rotational movement of soil particles. It is true that the deformation of any granular material is characterized by independent rotation of each particle. Then, it is imperative for us to introduce couple stress into the mechanics of granular material. So far, however, couple stress has been introduced only in elastic material (Mindlin,¹⁴ Toupin²⁵). It is known that the tangential stress in a continuum endowed with couple stress is not symmetric. We believe that the mathematical methods — the theory of characteristic lines, the dyadic notation of tensors, and the geometric expression of tensors — that have been successfully used in this paper can be extended to the nonsymmetric system.

The second course is the introduction of the pore space distribution. Goodman and Cowin⁹ developed a mathematical concept of pore space distribution and introduced it into the frame of elasticity. In the contemporary soil mechanics, no rational method is employed to conceptually convert a collection of particles to a continuum. Goodman and Cowin's approach supplies an ideal correction to the traditional defect. Snow mechanics, which is characterized by extraordinarily large pore space, especially needs this correction. However, we do not know yet how plastic constitutive equations can be introduced in this new system.

Mandl and Luque,¹³ by citing Truesdell,²⁶ showed that in a general isotropic continuum the non-coaxiality of the principal axes of stress tensor and strain rate tensor occurs only during in-plane, but never during three-dimensional, deformation. In other words, to discuss the three-dimensional plastic deformation of the non-coaxial Coulomb material, we must determine a plane in which the in-plane deformation occurs. The in-plane deformation plane may develop fully or partially. The complexity of the deformation of the model we are proposing is, we hope, the exact reflection of the complexity of the actual three-dimensional deformation.

The three-dimensional yield criterion of the Coulomb material was given in Takagi²¹ by applying the theory of plastic potential, as a one-parameter continuum connecting Tresca's yield criterion and von Mises' yield criterion. It may be possible that, rather than giving a specific value to the parameter and picking up a specific three-dimensional yield criterion, the parameter of this continuum may be an additional unknown for describing the three-dimensional deformation of the Coulomb material.

LITERATURE CITED

1. Abbott, M.B. (1966) *An introduction to the method of characteristics*. New York: American Elsevier Publishing Co., Inc.
2. Brand, L. (1948) *Vector and tensor analysis*. New York: John Wiley and Sons, Inc.
3. Courant, R. and D. Hilbert (1962) *Methods of mathematical physics*, vol. II. New York: Interscience Publishers.
4. De Josselin de Jong, G. (1964) Lower bound collapse theorem and lack of normality of strain rate to yield surface for soils. *Rheology and Soil Mechanics Symposium, Grenoble*, p. 69-78, Berlin: Springer.
5. Drucker, D.C. (1951) A more fundamental approach to plastic stress-strain relation. *Proceedings, First U.S. National Congress for Applied Mechanics*, American Society of Mechanical Engineers, p. 487-491.
6. Drucker, D.C. (1967) *Introduction to mechanics of deformable solids*. New York: McGraw-Hill Book Co.
7. Drucker, D.C. and W. Prager (1952) Soil mechanics and plastic analysis or limit design. *Quarterly of Applied Mathematics*, vol. 10, p. 157-165.
8. Geniev, G.A. (1958) *Voprosy Dinamiki Sypuchei Sredy*. Akademiia Stroitel'stva i Arkhitektury SSSR, Moscow.
9. Goodman, M.A. and S.C. Cowin (1972) A continuum theory for granular materials. *Archive of Rational Mechanics and Analysis*, vol. 44, p. 249-266.
10. Haythornthwaite, R.M. (1963) The kinematics of soils. In *Progress in Applied Mechanics*. New York: The MacMillan Co., p. 235-250.
11. Hill, R. (1949) The plastic yielding of notched bars under tension. *Quarterly Journal of Mechanics and Applied Mathematics*, vol. 2, p. 40-52.
12. Mandl, J. (1964) Conditions de stabilité et postulat de Drucker. *Rheology and Soil Mechanics Symposium, Grenoble*, p. 58-68, Berlin: Springer.
13. Mandl, G. and R.F. Luque (1970) Fully developed plastic shear flow of granular materials. *Geotechnique*, vol. 20, p. 277-307.
14. Mindlin, R.D. (1963) Influence of couple-stresses on stress-concentrations. *Experimental Mechanics*, vol. 3, p. 1-7.
15. Prager, W. and P.G. Hodge (1951) *Theory of perfectly plastic soils*. New York: John Wiley and Sons, Inc.
16. Sedov, L.I. (1962) *Introduction to the mechanics of a continuous medium*. Originally published as: *Vvedenie V Mekhaniku Sploshnoi Sredy*, State Physics and Mathematics Press, Moscow, 1962. Translation published in 1965 by Addison-Wesley Publishing Co. Inc., Reading, Mass.
17. Shield, R.T. (1953) Mixed boundary value problems in soil mechanics. *Quarterly of Applied Mathematics*, vol. 11, p. 61-75.
18. Sokolovski, V.V. (1960) *Statics of soil media*. London: Butterworth.
19. Takagi, S. (1958, 1959, 1960) Lectures on soil mechanics, Parts I-VIII: *Journal, Agric. Engrg. Soc. of Japan*, Tokyo, Japan. Part I: vol. 26, no. 4, 1958, p. 58-63; Part II: vol. 26, no. 5, 1958, p. 41-45; Part III: vol. 26, no. 6, 1959, p. 50-55; Part IV: vol. 27, no. 1, 1959, p. 44-49; Part V: vol. 27, no. 2, 1959, p. 49-54; Part VI: vol. 27, no. 3, 1959, p. 38-44; Part VII: vol. 27, no. 4, 1959, p. 43-50; Part VIII: vol. 27, no. 6, 1960, p. 37-44 (in Japanese).
20. Takagi, S. (1962) Plane plastic deformation of soils. *Journal of Engineering Mechanics Division, Proceedings of American Society of Civil Engineers*, vol. 88, no. EM3, p. 107-151.
21. Takagi, S. (1965) Three-dimensional yield criterion of $c-\phi$ material. CRREL Research Report 179. AD 629875.
22. Takagi, S. (1968) *The Gibbs-Einstein tensor analysis with application to continuum mechanics and canonical forms of general second-order tensors*. *Recent Advances in Engineering Science*, vol. 3, New York: Gordon and Breach.

23. Takagi, S. (1973) Theory of soil plasticity with indefinite angle of non-coaxiality. CRREL Research Report 307. AD 762560.
24. Terzaghi, K. (1943) *Theoretical soil mechanics*. New York: J. Wiley and Sons.
25. Toupin, R.A. (1964) Theories of elasticity with couple-stress. *Archive for Rational Mechanics and Analysis*, vol. 17, no. 85, p. 112.
26. Truesdell, C. (1961) The principle of continuum mechanics. Colloquium lectures in pure and applied sciences, p. 82-85. No. 5 Field Research Laboratory, Socony Mobile Oil Co., Dallas, Texas.
27. Wilson, E.W. (1960) *Vector analysis*. Founded upon the lectures of J.W. Gibbs. New York: Republication by Dover Publications Co., Inc.
28. Yoshimura, Y. (1957) *Sesei-rikigaku* (Theory of plasticity). Tokyo: Kyoritsushuppan K.K. (In Japanese.)

U.S. GOVERNMENT PRINTING OFFICE: 1977-702-598/22